Thermoelectric power of aligned and randomly oriented carbon nanotubes

M. Baxendale, K. G. Lim,* and G. A. J. Amaratunga
Cambridge University Engineering Department, Trumpington Street, Cambridge CB2 1PZ, United Kingdom
(Received 28 October 1999)

Thermoelectric power was used to elucidate the electrical transport properties of aligned and randomly oriented carbon nanotube systems in the temperature range 77–450 K. A weakly negative thermoelectric power, comparable with that of a graphite flake, was observed for a macroscopic bundle of multiwall carbon nanotubes with individual axes aligned parallel to the main axis. However, mats of randomly oriented multiwall carbon nanotubes gave a strongly positive thermoelectric power, as did mats of single-wall nanotubes. This is evidence of the importance of intertube contacts in the interpretation of the thermoelectric power data for carbon nanotube systems. Models for thermoelectric power behavior incorporating contact effects are described.

Carbon nanotubes continue to attract much research interest due to their unique electrical properties and potential applications. Thermoelectric power (TEP) measurements have been used to elucidate the electronic properties of multiwall nanotube (MWNT) bundles and single-wall nanotube (SWNT) ''mats.'' [1] In both cases positive and moderately large TEP's with unusual temperature dependencies that approach zero as $T \rightarrow 0$ are observed in the range 0–300 K. Hone *et al.* observe similar TEP characteristics for sintered and unsintered SWNT mat samples and conclude that the measured TEP is an intrinsic property of the constituent nanotubes.[1] Tian *et al.* tacitly assume the TEP of a MWNT bundle is similarly intrinsic.[1] The aim of this work is to show that this positive TEP is not an intrinsic property of the nanotubes but rather is a consequence of random orientation of intertube contacts relative to the thermal gradient employed in the measurement. The temperature variation of diffusion TEP for randomly oriented nanotube systems is not that of a simple metal or semiconductor, nor is a power-law dependence observed—a signature of the variable range hopping (VRH) regime. This unusual TEP has been interpreted in terms of a variation of the Nordheim-Gorter relation for parallel metallic and semiconducting pathways.[1] Here results are interpreted in terms of the fibrillar conducting path model of Kaiser.[2]

The MWNT bundles used in this study produced by cathodic arc deposition are described elsewhere.[3] The material comprises aligned MWNT's close packed into bundles of outer diameter several tens of nanometers. These bundles in turn form bigger fiberlike structures of length 1–3 mm and approximate diameter 100 μm with individual MWNT axes aligned parallel to the main axis. These macroscopic structures exhibit a high degree of alignment, as evidenced by the observation of electronic quantum transport properties normally associated with single-mesoscopic structures.[4] The fiberlike structures were first heated in air at 700 °C to remove a thin overcoating of graphitic flakes and amorphous carbon. MWNT mats were produced by first grinding the fiberlike structures, dispersing the ground material in twice micellar-concentration sodium dodecyl sulfate solution, and standing in an ultrasound bath to form a suspension. The suspensions were left for several days during which any large fragments of material collected in the sediment. The liquid phase was then centrifuged at 5000 rpm for 10 min to extract macroscopic particles, filtered using a 0.4 μm pore size, and finally washed in distilled water. The MWNT-containing deposit was then scraped from the filter membrane, shaped into a 1 mm$\times$3 mm$\times$100 μm bar across the electrical contacts on the temperature-controlled platform of the TEP measurement system, and allowed to dry. A similar-sized sample was prepared for conductivity measurements and electrical contacts made by silver paste in the conventional four-contact configuration. SWNT's used in this study were produced by the cathodic arc deposition method.[5] Purification of the SWNT-containing material was by the method of Tohji *et al.*[6] The material was finally filtered and mats prepared by the method described above.

The cathodic arc deposition process for both MWNT and SWNT samples produces nanotubes with a distribution of electronic structure ranging from the semiconductor to metallic. For this reason the TEP of macroscopic nanotube mats has been modeled as parallel semiconducting and metallic pathways.[1]

TEP measurements were performed with a MMR technologies SB-100 Programmable Seebeck Controller unit.

For a homogeneous medium and energies close to the Fermi energy E_F, TEP is given by the standard Mott formula:[7]

$$S = \frac{\pi^2 k^2 T}{3e} \left. \frac{d \ln \sigma(E)}{dE} \right|_{E_F}, \tag{1}$$

where k is the Boltzman constant, T is temperature, e electronic charge, and $\sigma(E)$ a conductivitylike function of electron of energy E.

For heterogeneous media comprising fibrillar current paths, TEP is given by analogs of the Nordheim-Gorter rule for metallic diffusion TEP in the presence of different scattering mechanisms.[7] In the following analyses it is assumed that heat current follows the same fibrillar path as electrical current. By inserting the total conductivity of two pathways 1 and 2, $\sigma = \sigma_1 + \sigma_2$, into Eq. (1), (i) for a medium comprising parallel two-type current paths,

$$S=\frac{\sigma_1}{\sigma}S_1+\frac{\sigma_2}{\sigma}S_2, \tag{2}$$

where S_1, S_2 are their respective TEP's; (ii) for a medium comprising a fibrillar current path intermittently broken by series-connected ''barrier'' regions,

$$S=\frac{\Delta T_1}{\Delta T}S_1+\frac{\Delta T_2}{\Delta T}S_2 \tag{3}$$

where $S_i=\Delta V_i/\Delta T_i$ is the characteristic TEP produced by a temperature difference ΔT_i, V_i is the voltage drop across region i, and ΔT is the temperature gradient across the entire sample. If the barrier regions are randomly oriented relative to ΔT and the Wiedemann-Franz law holds, that is, electrical resistance is proportional to thermal resistance,

$$S=\frac{R_1}{R}S_1+\frac{R_2}{R}S_2, \tag{4}$$

where R_1 is the resistance of the fibrillar path, R_2 the resistance of the barrier region, $R=R_1+R_2$ the total resistance of the pathway, and S_1, S_2 are the TEP of the fibrillar pathway and barrier regions, respectively. If, however, the barrier regions are oriented perpendicular to the temperature gradient ΔT, the barrier region will lie on an isotherm, hence $\Delta T_2=0$ and Eq. (4) will reduce to

$$S=S_1. \tag{5}$$

In this case TEP is determined entirely by the fibrillar path with no contribution from the barriers even though the barriers may make a significant contribution to electrical resistance. Previous studies have tacitly assumed intertube barriers are negligible and Eq. (2) applied for parallel metallic and semiconducting pathways.[1]

Comparison of the TEP's of oriented and randomly dispersed systems can be achieved with the MWNT bundle and mat samples, respectively. Although the TEP of MWNT's may be complicated by interlayer interactions, such a comparison using SWNT's is not possible because macroscopic samples of aligned SWNT's are not available at present.

The temperature variation of normalized electrical resistance for the three samples used in this experiment is given in Fig. 1. The abrupt changes in resistivity for the mat samples at high temperature is an indication of the fibrillar nature of the current path: steps occur when current is rerouted by thermal expansion of the sample. Within this temperature range the resistance of the MWNT mat is essentially constant, that of the MWNT bundle is weakly semiconductorlike but does not have the temperature dependence of any common conduction mechanism, indicating that both MWNT samples have mixed-conductivity mechanisms.[8] However, the resistance of the conceptually simpler SWNT mat obeys the Mott expression for VRH, $\sigma=\sigma_0\exp[-(T_0/T)^{1/4}]$, as shown by the linearity of Fig. 1(b).

The TEP data for each sample and that for the in-plane TEP of a high-quality pyrolitic graphite flake in the temperature range 77–425 K are given in Fig. 2. Clearly there is a dramatic difference between the MWNT bundle and mat samples. The TEP of the aligned MWNT bundle sample is weakly negative and comparable with that of graphite

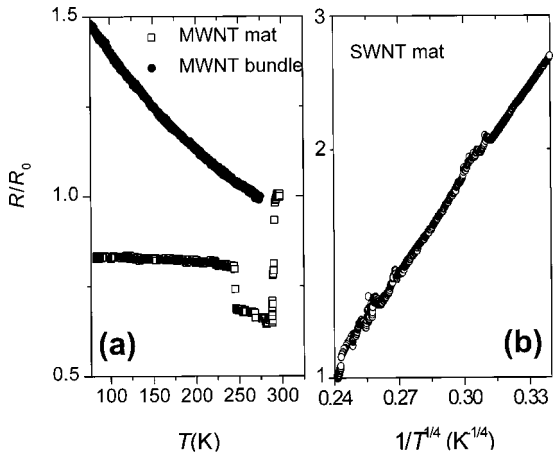

FIG. 1. Temperature variation of normalized resistance for (a) the MWNT bundle and mat samples, and (b) SWNT mat, from this plot $T_0=7000$ K.

whereas that of the MWNT mat is strongly positive, as is that for the SWNT mat. The sign and magnitude of the TEP of the mat samples are comparable with previously reported data.[1] Since the MWNT bundle and mat used in the measurement are taken from the same source material they are expected to contain nanotubes with the same distribution of electronic properties. Therefore, there are two possible explanations for the difference of the MWNT mat and bundle TEP behavior: either the orientation of the intertube contacts relative to ΔT is critical, or the mechanical deformation of individual nanotubes in a random network significantly alters their electronic structure. Recent calculations by Nardelli show that SWNT's maintain their basic electrical properties even in the presence of large mechanical deformations.[9] Since their electrical and thermal properties are likely to be determined by the outer layer it is reasonable to assume that the same is true for MWNT's. The recent observation of the Aharonov-Bohm effect in a single MWNT is convincing proof that the electric current flows in the outermost graphene sheet only, at least at low temperature $T<70$ K.[10]

In the case of the MWNT bundle, the intertube barriers are perpendicular to ΔT so the measured TEP is that of the nanotube conducting pathways according to Eq. (2), which can be justifiably modeled as parallel semiconducting and metallic components. Assuming the absence of phonon-drag effects in the temperature range of the measurement, the metallic diffusion TEP in the phonon scattering regime using the free-electron approximation is[7]

$$S_1=\frac{\pi k^2}{eE_F}T. \tag{6}$$

That for a nondegenerate semiconductor is

$$S_2=\frac{k}{e}\left[\frac{|\lambda|}{T}+\beta\right], \tag{7}$$

where λ is the gap temperature measured from the midgap to the band edge and β is a constant. In Eqs. (6) and (7), electron and hole transport is indicated by negative and positive signs, respectively.

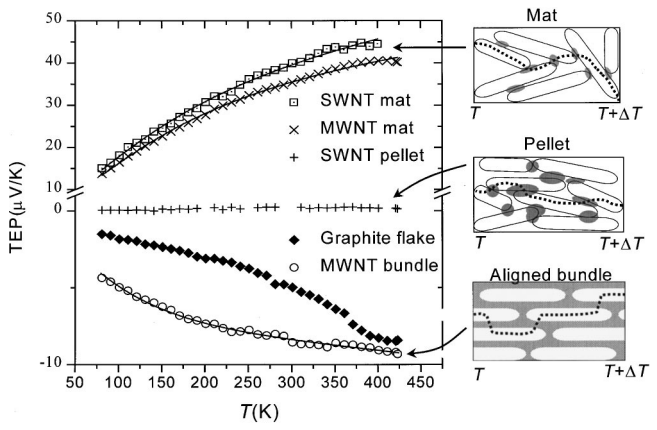

FIG. 2. Temperature variation of TEP for the various nanotube samples and that of in-plane TEP of high-quality pyrolitic graphite. Solid lines are the fits to the models described in the text. The schematic diagrams to the right of the plot are 2D representations of the nature of the thermal current paths (dotted lines) for the aligned nanotube bundle, mat, and pellet samples in the TEP measurement. The spatial extent of intertube barriers is schematically indicated by the gray areas.

PARALLEL METALLIC AND SEMICONDUCTING PATHWAYS

If the conductivity of the semiconductor path $\sigma_2 \propto \exp(-\lambda/T)$, and the metallic conductivity is σ_1, general expressions can be derived from Eq. (2) where *A, B,* and *C* are constants.

(i) $\sigma_1 = \text{const}$, $\sigma_1 \gg \sigma_2$,

$$S = AT + \left[\frac{B\lambda}{T} + C\right]\exp\left(\frac{-\lambda}{T}\right). \tag{8}$$

(ii) $\sigma_1 \propto 1/T$, $\sigma_1 \gg \sigma_2$,

$$S = AT + [BT + CT]\exp\left(\frac{-\lambda}{T}\right). \tag{9}$$

(iii) σ_1 is a const, $\sigma_1 \ll \sigma_2$,

$$S = A\exp\left(\frac{\lambda}{T}\right) + \left[\frac{B\lambda}{T} + C\right]. \tag{10}$$

(iv) $\sigma_1 \propto 1/T$, $\sigma_1 \ll \sigma_2$,

$$S = \frac{A}{T}\exp\left(\frac{\lambda}{T}\right) + \left[\frac{B\lambda}{T} + C\right]. \tag{11}$$

The first and second terms in Eqs. (8)–(11) represent the weighted contributions of metallic and semiconducting TEP's, respectively.

The MWNT bundle TEP data in Fig. 2 can be fitted to equations of the form Eqs. (8)–(11) by a procedure that requires *B* and *C* to be of the same sign—as is required in Eq. (7)—and λ to have a physically reasonable value. Adequate fitting of the data to Eqs. (8)–(11) using the actual form of σ shown in Fig. 1 and the various forms of σ_1 and σ_2 outlined above can be also achieved.

The best fits are achieved with Eqs. (8) and (9) with values of $A-C$, λ given in Table I and are shown as a solid line in Fig. 2. The signs of $A-C$ indicate electronlike metallic TEP, holelike semiconductor TEP, and the magnitudes λ correspond to very narrow energy gaps energy of 6 and 20 meV. Since all the forms Eqs. (8)–(11) give reasonable fits to the data and that some degree of misalignment will give rise to a positive component of TEP, direct interpretation of the fitting parameters in terms of the electronic structure of the individual nanotubes is likely to lead to false conclusions. At best it can be said that some form of parallel conduction path model can describe the TEP of the MWNT bundle. Since there is no contribution to TEP from intertube barriers, the weakly negative characteristic of the MWNT bundle, not the positive TEP of the randomly oriented mats, is likely to be the intrinsic property of the nanotube system.

TABLE I. Best fits parameter values achieved with Eqs. (8) and (9) for $A-C$, λ.

	A (μV/K^2)	B	C	λ (K)
Eq. (8)	−13.3	28.8 μV/K	2.2 μV/K	57
Eq. (9)	−0.057	3×10^{-5} μV/K^2	0.06 μV/K^2	201

A strongly positive TEP is measured for the mat samples: this is consequence of the random distribution of intertube barriers relative to ΔT for the reasons described above. Hence, the TEP for a mat is best modeled as a pathway of semiconducting nanotubes broken by series-connected intertube barriers, in parallel with a similar metallic pathway. Electrical conductivity through the barrier region is likely to be by hopping—the VRH conduction is present in the SWNT mat sample, see Fig. 1(b), and is likely to be a component of the MWNT mat conductivity.

In the VRH regime[7]

$$S_h = \frac{k^2}{2e}(T_0 T)^{1/2}\left.\frac{d\ln\sigma(E)}{dE}\right|_{E_F}, \tag{12}$$

where T_0 is the parameter contained in the 3D VRH conductivity expression, $\sigma = \sigma_0 \exp[-(T_0/T)^{1/4}]$; the sign of S_n indicates the carrier type.

PATHWAY OF METALLIC FILAMENTS BROKEN BY SERIES-CONNECTED BARRIERS IN PARALLEL WITH A SIMILAR SEMICONDUCTING PATHWAY

The series combination of pathway and barrier was modeled using Eq. (3), and combined with Eq. (2) to describe the parallel connection of metallic and semiconducting pathways. The equations below assume $R_b \gg R_m, R_s$ where R_b is the barrier resistance and R_m, R_s the resistance of a metallic and semiconducting nanotube, respectively, and $A'-E$ are constants. Here conductivity through the barrier is by 3D VRH: the form of R_b is derived from the expression for conductivity and the contribution of the barrier to TEP is given by Eq. (12).

(i) $R_m = $ const,

$$S = A'T\exp\left(\frac{-T}{T_0}\right)^{1/4} + B'\exp\left(\frac{-\lambda}{T}\right) \times \exp\left(\frac{-T}{T_0}\right)^{1/4}\left[\frac{C'\lambda}{T} + D\right] + ET^{1/2}. \tag{13}$$

TABLE II. Best fit parameter values achieved with Eqs. (13) and (14) for $A-E$, λ.

	A'	B'	C' (μV/K)	D (μV/K)	B (μV/K$^{3/2}$)	λ (K)
MWNT mat: Eq. (13)	-0.019 μV/K^2	625	*3×10−5*	*0.06*	1.32	201
MWNT mat: Eq. (14)	-2×10^{-5} μV/K^3	560	*3×10−5*	*0.06*	1.21	201
SWNT mat: Eq. (13)	-0.007	616	*3×10−5*	*0.06*	1.37	201
SWNT mat: Eq. (14)	-8×10^{-6}	601	*3×10−5*	*0.06*	1.32	201

(ii) $R_m \propto T$,

$$S = A'T^2 \exp\left(\frac{-T}{T_0}\right)^{1/4} + B'\exp\left(\frac{-\lambda}{T}\right) \times \exp\left(\frac{-T}{T_0}\right)^{1/4}\left[\frac{C'\lambda}{T} + D\right] + ET^{1/2}. \quad (14)$$

The first, second, and third terms in Eqs. (13) and (14) represent the weighted contributions of metallic, semiconducting, and hopping TEP's, respectively.

Equations (13) and (14) were fitted to the mat TEP data using the semiconductor gap temperature λ and the intrinsic constants of semiconducting TEP, B and C, found in the fitting of the MWNT bundle data to Eq. (9)—inserted into the equations as constants C' and D (italicized in Table II)—and A', B', and E varied. The intrinsic metallic TEP, A, that from Eq. (6) equals $\pi k^2/eE_F$, cannot be inserted in the same way because A' contains unknown geometric factors that enter Eqs. (13) and (14) via R_m. The value of $T_0 = 7000$ K is determined from the SWNT mat conductivity data, Fig. 1(b). The best fit parameter values are given in Table II: both Eqs. (13) and (14) gave identical quality fits as indicated by the solid lines in Fig. 2.

Comparable quality fits, with parameters of the same sign, can be achieved with the values of C', D and λ from the fitting of Eq. (8) to MWNT bundle data so it would be wrong to quantitatively interpret the above values. However, it can be concluded that the measured mat TEP can be qualitatively described in terms of the above model with an electronlike metallic component, a holelike semiconductor component, and a holelike hopping component. The change of sign of TEP when the nanotubes are randomly dispersed is caused by the introduction of the $\exp(-T_0/T)^{1/4}$ factors and the positive hopping term $ET^{1/2}$ in the form of total TEP. Further evidence of this analysis was obtained from the TEP of a SWNT pellet sample made by applying several MPa to a SWNT mat (Fig. 2). In pellet form the intertube contact area is increased relative to a mat so the probability of intertube hopping along an isotherm is greatly increased. This is seen as a TEP intermediate between the aligned and randomly oriented TEP behaviors.

In contrast to the results reported here, Tian *et al.* have reported a positive TEP for a MWNT bundle.[1] We speculate that this due to a lower degree of nanotube alignment in their bundle, giving rise to positive TEP components. In this sense TEP can be viewed as an indicator of the quality of nanotube alignment. We measured the TEP of several other MWNT bundles and found them all to be weakly negative although some had more positive components than that of the bundle in Fig. 2. The source of the positive TEP components could be either intrinsic or due to poorer quality of nanotube alignment. Thermal cycling of these bundles tended to lessen the positive components suggesting that this was due to some disorder being annealed out of the conducting pathway. The MWNT bundle TEP shown in Fig. 2 was unchanged by thermal cycling, and therefore assumed to be that of an entirely intrinsic conduction process. There was little sample-to-sample variation of mat TEP's as is to be expected in the presence of random orientation.

In conclusion, the TEP of aligned and randomly oriented nanotube systems are of different sign and magnitude because the orientation of intertube barriers relative to ΔT is significant. When these barriers are aligned perpendicular to ΔT, intertube hopping occurs along an isotherm so they provide no contribution to the total TEP, which is weakly negative. However, if these barrier regions are randomly oriented, significant positive components of TEP are introduced and the total becomes strongly positive. This effect must be included in the interpretation of TEP for nanotube systems and a model is proposed. TEP measurements can be used to probe the degree of alignment in nanotube systems.

*Present address: Department of Electrical Engineering and Electronics, University of Liverpool, Liverpool L69 3GJ, U.K.

[1] M. Tian, L. Chen, F. Li, R. Wang, Z. Mao, and Y. Zhang, J. Appl. Phys. **82**, 3164 (1997); J. Hone, I. Ellwood, M. Munro, A. Mizel, M. L. Cohen, and A. Zettl, Phys. Rev. Lett. **80**, 1042 (1998).
[2] A. B. Kaiser, Phys. Rev. B **40**, 2806 (1989).
[3] X. K. Wang, X. W. Lin, V. P. Dravid, J. B. Ketterson, and R. P. H. Chang, Appl. Phys. Lett. **62**, 1881 (1993).
[4] M. Baxendale, V. Z. Mordkovich, S. Yoshimura, and R. P. H. Chang, Phys. Rev. B **56**, 2161 (1997).
[5] P. Bernier, W. Maser, C. Jouret, A. Loiseau, M. L. de la Chapelle, S. Lefrant, R. Lee, and J. E. Fischer, Carbon **36**, 675 (1998).
[6] K. Tohji, H. Takahashi, Y. Shinoda, N. Shimizu, B. Jeyadevan, I. Matsuoka, Y. Saito, A. Kasuya, S. Ito, and Y. Nishina, J. Phys. Chem. B **101**, 1974 (1997).
[7] R. D. Bernard, *Thermoelectricity in Metals and Alloys* (Taylor & Francis, London, 1992).
[8] A. B. Kaiser, G. Düsberg, and S. Roth, Phys. Rev. B **57**, 1418 (1998).
[9] M. B. Nardelli, Phys. Rev. B **60**, 7828 (1999).
[10] C. Schönenberger, A. Bachtold, C. Strunk, J.-P. Salvetat, and L. Forró, Appl. Phys. A: Mater. Sci. Process. **69**, 283 (1999).